Ten percent of Halon 1301 will not extinguish an established A-50 pool fire or a flame propagating through a rich vapor/air mixture such as might occur in unventilated compartment. However, it will extinguish secondary fires ignited by such events.

References

[1] Amendment 2, Feb. 1964, Military Specification MIL-P-27402 (USAF), Aug. 1961, Air Force Rocket Propulsion Lab.

[2] Mignotte, P., "Thermodynamic and Physiochemical Study of Mixtures of Hydrazine with Unsymmetrical Dimethylhydrazine," *Revue de l'Institut Francais de Petrole*, Vol. 8, 1963, pp. 1–54.

[3] *International Critical Tables*, McGraw-Hill, N. Y., Vol. 5, 1929, p. 54.

[4] Henderson, W. P., private communication, Edgewood Arsenal, March 1968.

[5] Jost, W., *Diffusion in Solids, Liquids and Gases*, Academic Press, New York, 1952.

[6] Zabetakis, M. G., Scott, G. S., and Jones, G. W., "The Flammability Characteristics of the C_nH_{2n-6} Aromatic Series," Report of Investigations 4824, 1951, Bureau of Mines.

[7] Litchfield, E. L. and Furno, A. L., "Flammability of Propellant Combinations," Annual Report 1, Aug. 1964–June 1965, Government Order H-76708, prepared for George C. Marshall Space Flight Center, NASA, Huntsville, Ala.

[8] Lewis, B. and von Elbe, G., *Combustion, Flames, and Explosions of Gases*, 2nd ed., Academic Press, New York, 1961, p. 381.

[9] Rosser, W. A., Wise, H., and Miller, J , *Seventh Symposium (International) on Combustion*, Butterworths, London, 1958, pp. 175–182.

[10] Burgess, D. and Zabetakis, M. G., "Fire and Explosion Hazards Associated with Liquefied Natural Gas," Report of Investigations 6099, 1962, Bureau of Mines.

[11] "A Study of Extinguishment and Control of Fires Involving Hydrazine-Type Fuels with Air and Nitrogen Tetroxide," TR ASD-TR-61-716, May 1962, Flight Accessions Lab., Wright-Patterson Air Force Base, Ohio.

[12] *Titan II Storable Propellant Handbook*, AFBSO-TR-62-2, Bell Aerosystems Co., Buffalo, N. Y.

NOVEMBER 1969 J. SPACECRAFT VOL. 6, NO. 11

Refined Measurements of Exhaust-Plume-Induced Radar Amplitude and Phase Noise

J. W. WILLIAMS*
Lockheed Propulsion Company, Redlands, Calif.

AND

L. D. SMOOT†
Brigham Young University, Provo, Utah

A new facility for measuring plume-induced radar attenuation and noise is described. Three solid-propellant motor firings were conducted and measurements of *X*- band attenuation and *X*-band AM and PM noise are reported. Influences of sideband frequency and plume position on noise levels are shown. Peak attenuation level for this highly aluminized propellant was approximately 12–15 db. Maximum noise levels, like attenuation, occurred in the afterburning regions of the plume and showed a strong dependence on plume position. Near the nozzle exit plane, the amplitude noise in a 500-Hz bandwidth, 1 kHz from the CW, *X*-band carrier was about 37 dbc. At aft regions of the plume, the attenuation and amplitude noise levels increased about 3 and 10 db, respectively. Phase noise levels were comparable to the amplitude noise levels. Results of this test series were compared with data reported previously for nearly identical propellant/motor systems. Attenuation and AM noise measurements agreed well with earlier tests, but PM noise measurements were higher than those previously reported. These new data are considered more accurate because of the careful attention given to facility calibration and to elimination of acoustically induced noise.

Introduction

IN a previous publication, Smoot and Seliga[1] reported amplitude- (AM) and phase-modulated (PM) noise levels that were induced on an *X*-band radar signal that traversed a rocket exhaust plume. These data were the first measurements of this type that were known to have been published in the open literature. Reported levels of AM noise were substantially higher than those for PM noise. However, PM noise levels showed wide excursions during each test firing. The authors noted: "It is doubtful that the PM levels shown were significant, except for the 18% aluminized propellant."

This paper describes a new facility for measuring plume-induced radar attenuation and noise. Three motor firings have been conducted using one of the propellant formulations, the same hardware, and essentially the same conditions as the previous tests. These newer attenuation and AM noise measurements agree well with earlier measurements, but PM noise data are substantially different.

Experimental Program Plan

Microphonic interference caused by the severe acoustic environment on the modified *X*-band circuitry was investigated during the first firing. In the second and third firings, exhaust plume induced *X*-band attenuation and *X*-band AM

Received March 7, 1969; revision received July 11, 1969.

* Research Engineer.

† Associate Professor of Chemical Engineering. Member AIAA.

and PM noise were measured. Both the exit plane and downstream regions of the exhaust were investigated during these two firings.

The same Nitroplastisol propellant formulation containing 18% aluminum (propellant 1 in Table 1 of Ref. 1) was used for all three motors. The test motor was a standard, 3000-lb thrust heavy-wall motor with a 1-in. throat diameter and expansion ratio of 7.4. No measurements of potassium and sodium level were made on these propellants. However, previous measurements on an identical propellant showed that the formulation contained about 25-ppm K and 137-ppm Na.

The transverse measurements were made at X-band (9.54 GHz) frequency with focused-beam systems. A moving microwave cart (Fig. 1) permitted the investigation of radar attenuation vs plume position. Dielectric lenses focus the plane, polarized signal at a point midway between the receiving and transmitting horns. This focused region coincides with the nominal centerline of the plume and persists in the transverse direction for approximately 8 in. before noticeable beam divergence occurs. The microwave beam configuration throughout this region is elliptically shaped with the major and minor axes corresponding respectively to the directions of the electric (E) and magnetic (H) field vectors. At the 3-ft horn separation used in these tests, the X-band beam diameters to the -3 db points in the E and H directions are $3\frac{1}{2}$ and 2 in., respectively. Also, a transverse magnetic (TM) signal polarization with the E vector parallel to the exhaust plume and ground plane was used.

The moving cart, mounted on two fixed rails, enables the spatial dependence of AM/PM noise and attenuation on plume position to be determined. A base framework holds the microwave and electronic circuits, while the lens-corrected horn antennas are positioned around the 10-ft-diam octagonal ring. To provide the 3-ft X-band horn separation, a rigid framework is used that extends the horns toward the center of the 10-ft ring. Cart motion is provided by a high-pressure, hydraulic propulsion system. For this sequence of firings, typical programed cart velocity was 12 fps. Cart position as a function of firing time was determined by an electromechanical switch on a wheel. Effect of firing time on exhaust-plume radar attenuation and noise was obtained by keeping the cart stationary at a selected position downstream from the nozzle exit plane.

Measurement Systems and Technique

Figure 2 shows the basic microwave detection circuits. The microwave system was specifically designed for compatibility with the moving cart, motor test stand, and track apron. Radar transmission to and from the antenna was made with standard rectangular waveguide components. Specific design requirements for this system were low klystron residual AM/PM noise, high receiver sensitivity, and system frequency stability.

The X-band system shown in Fig. 2 is basically a phase-locked continuous wave interferometer. Both the transmitter and local oscillator reflex klystrons are phase-locked to a very stable 30-MHz reference source. However, instead of comparing a "clean" portion of the transmitted signal with the affected signal, as is usually done in interferometer systems (for example, Ref. 1), a 30-MHz reference oscillator phase-lock technique was used. Here, both the transmitter

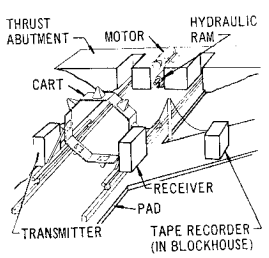

Fig. 1 Schematic of microwave-exhaust-plume interference facility.

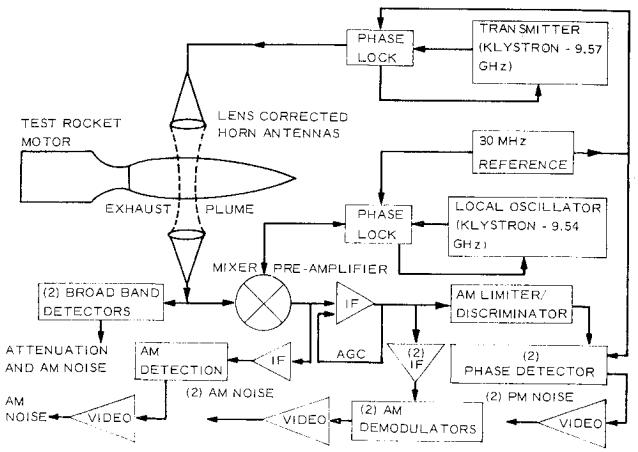

Fig. 2 Coherent source interfereometer for exhaust-plume radar noise and attenuation measurements.

klystron and local oscillator klystron are phase-locked to this common reference source. Furthermore, since the phase-lock system was designed to permit transmission from the two signal sources only when they differed by 30 MHz, the two signals when mixed result in a clean intermediate frequency (IF) of 30 MHz. This occurs only when the transmitted signal is not changed by the exhaust plume. When exhaust-plume effects are significant, a noisy IF signal results. This signal is both attenuated by its transmission through the absorbing plume and phase and amplitude-modulated by changes in the refractive index of the plume.

The AM noise sideband levels for frequencies greater than 500 Hz were obtained from the preamplified IF signal at stages before and after the automatic gain control (AGC) loop. A 2-MHz bandwidth IF amplifier with a video amplifier-cathode follower is used for the AM demodulation of the signal before the AGC stage. This system is similar to two other rectifier-type demodulators that follow the AGC loop. The use of the three IF amplifier-video demodulators improves system reliability and enables the amplifier gains to be staggered, thus preventing excessive AM noise levels from saturating the test data. For frequencies less than about 500-Hz, amplitude detection by crystal video detectors that directly rectify the microwave current were used. The crystal detectors have almost a flat frequency vs signal response for AM video frequencies to 100 kHz. The two systems for AM detection were necessary to avoid the smoothing effect of the slow AGC circuit at the lower frequencies. Attenuation or amplitude measurements of the d.c. component also were performed with the video crystal detectors.

Phase modulation levels are obtained from an IF signal that is essentially free from AM effects because of the AGC loop and further AM discriminating-limiting in the receiver. Video phase demodulation occurs when the original coherent reference source is compared in a phase bridge system of the ring modulator design. The diode pairs that comprise the modulator when subjected to the initial clean reference signal and the noisy-plume signal result in the useful PM video signal. Strictly, this signal is related to the sine of the phase difference between the two IF inputs. However, for the small phase shift levels caused by these exhaust plumes, the sine of the phase shift and the measured phase change are essentially equal and this difference is negligible. The video outputs are amplified by wide-band flat response amplifiers with band limits from 5 Hz to 1 MHz. Two identical systems are used to assure system reliability.

Several sources of unwanted noise can affect the performance of the microwave system thereby reducing plume-induced noise detection capability. At this facility, noise created by acoustics of a rocket motor firing initially caused serious degradation of the PM video signal. Electronic modifications of the phase-lock circuits were required before this

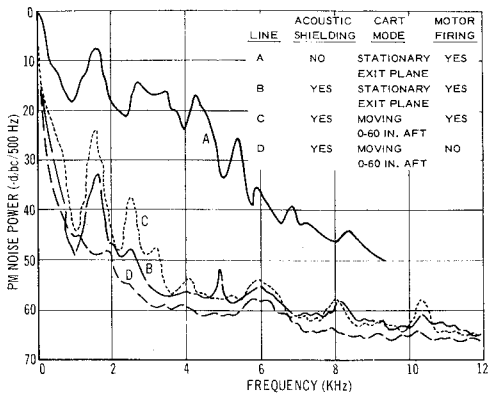

Fig. 3 Effect of acoustic noise with and without shielding on PM system performance.

source of interference was eliminated. Noise induced by the sled was observed only during its initial period of acceleration. Other sled motion effects were not important. The vibration effects of the two horns relative to one another that had previously[1] caused wide excursions in PM noise levels were eliminated through rigid construction of the octagonal ring which supports the horns. Inherent system noise levels during these tests depended on reference oscillator performance in the phase-lock circuits as well as correct operation of the other microwave and IF stages. Discrete PM sideband frequencies, as shown later, are observed on the PM spectra at modulation frequencies of about 5.5 kHz. These signals arise from a relatively large sideband on the reference oscillator phase-lock circuit and are present on the PM video spectra of the test firings.

Calibration and Data Recording and Analysis

Attenuation calibrations were obtained before each firing by varying a known precision, microwave attenuator. A comparison of the measured signal with the known microwave attenuator allowed precise attenuation measurements. Amplitude calibrations for the CW, *X*-band modulated or time-varying signals were performed with a microwave PIN modulator (a microwave power absorption device whose absorption is controlled by a negative bias voltage). A linear range between the negative bias voltage and the microwave absorption in decibels was first established. A 10-kHz sine wave of known zero-to-peak voltage was superimposed on this linear region of the modulation-absorption curve. The degree of modulation used was determined from the ratio between the difference of the trough and nominal voltages to the nominal voltage for the IF signal. Trough voltage depression of the IF signal was -0.125 db. This value was obtained from the product of the superimposed sine wave zero-to-peak voltage and the slope of the linear region of the absorption curve. The single sideband level in decibels below carrier (dbc) determined from these calculations was 43. Amplitude calibration was then made by changing this modulating voltage in known amounts and recording the results prior to each test on magnetic tape.

Phase modulation levels are obtained directly from the recorded signal. A constant 12-kHz frequency difference is established between the transmitter and local oscillator by adjusting the transmitter's phase-lock reference circuit such that the relative difference between the two signal sources is not 30 MHz but exactly 30.012 MHz. Instead of a d.c. signal that is not detected by the analyzers, this difference results in a low-frequency, 12-kHz carrier. Plume noise levels then appear as sidebands around this carrier and are read directly in decibels below carrier from the analyzer's data display system. To assure that the phase system was operating linearly, the transmitter's phase lock-reference circuit was modulated, thereby, causing frequency modulation of the transmitted signal. Since the shift of frequency due to the peak levels of the externally applied modulating signal were known, together with the modulating frequency, precise modulation indices were readily determined.‡ For indices less than about 0.1, the noise level can be obtained easily.§ Therefore, since deviation frequency is a direct function of the applied modulating signal amplitude, variation of the modulating voltage level in predetermined steps will change the sideband levels for small modulation indices by an identical amount. This procedure was used to verify the linearity of the phase circuits and the accuracy of the PM calibration technique described earlier.

The 14-channel magnetic tape recorder/reproducer used has reel-to-reel, reel-to-loop, or continuous loop operation modes. At a tape speed of 10 fps, the recorder has a flat response between d.c. and 600 kHz. The rms-to-rms signal/noise ratio at the 216-kHz center frequency is ~45 db. Signal functions recorded were the *X*-band AM and PM noise levels, *X*-band attenuation levels, *X*-band transmitter and local oscillator reference level monitors, cart position, and rocket chamber pressure.

The characteristics of the video noise sideband structure originally on the CW *X*-band carrier were determined with a spectral analysis system. The analyzer provides an automatic visual presentation of the power density (PSD) function of the complex noise signal. The resulting frequency/power spectra were obtained from the tape loops made of the entire motor burn period. A low statistical error was obtained in the integrated analysis of the random data by slowly scanning a 0.5-sec firing period with a 200-Hz band-pass filter for the frequency range from 500 Hz to 40 kHz and with a 20-Hz bandpass filter for the interval from 20 Hz to 4000 Hz. Signal reproduction from the continuous tape loops was at real-time speeds (10 fps).

Amplitude levels measured were referenced with respect to the average level of the attenuated carrier during the analysis period. Both amplitude and phase noise levels are reported for convenience in a 500-Hz bandwidth.

Test Results

Acoustic Interference

In preliminary tests of acoustic noise and mechanical effects on system performance, an undesirable level of acoustically induced PM noise was observed. The tests were made during rocket motor firings in both closed- and open-loop modes. In the first case, a direct link between transmitter and receiver was established by providing a waveguide for the transmission path. In the open-loop mode, the transmission path was by way of the lens corrected horns. In both instances no plume interference was possible during motor firing and cart motion.

A power spectral density (PSD) analysis (using an MB T-1000 Spectral Analyzer System) of the data collected during the acoustic test showed phase noise of similar magnitude and spectral distribution as had been measured during a radar-exhaust interference test. In other words, unwanted acoustically induced noise was seriously masking the desired PM noise levels. Subsequent investigation isolated the difficulty to the rf reference sources of the phase-lock circuits. (An increase in system noise level at low sideband frequencies also was observed in the AM circuits under the same severe acoustic environment, but the increase was small relative to the exhaust-induced AM noise.) Acoustic shielding of the microphonic rf signal sources was accomplished removing the

‡ The modulation index (maximum phase shift, rad) is given by $\Delta f/f_m$, where Δf is the peak deviation (Hz) and f_m the modulating frequency (Hz).

§ For modulation levels less than 0.1, the level of FM noise is given by db = $20 \log(2f_m/(\Delta f))$.

Table 1 Radar-exhaust plume interference test parameters

Motor No.	Attenuation X band (9.57 GHz)	Single sideband noise, kHz[a] AM	PM	Burn time, PM	Cart mode	Analysis period (sec after ignition)
2	d.c. to ~10 Hz	0.5–20	0–20	0.96	Stat.[b] 0–0.32 in. Mov.[c] 13.5–70.5 in.	0.05–0.55 0.5–1.0
3	d.c. to ~10 Hz	0.5–20	0–20	0.99	Stat. 72 in. aft	0.05–0.55 0.4–0.90

[a] Attenuation and noise recorded for stationary and moving portions of test.
[b] Stationary from motor ignition (t = 0 sec) to time t, sec.
[c] Moving during motor burn time for the distance, indicated in inches, from nozzle exit plane.

reference circuits from the two oscillator synchronizers and placing them in an acoustically shielded box in the instrumentation blockhouse, ~40 ft from the nozzle exit plane.

A motor firing was then made using the open-loop configuration for the propagation path. Figure 3 presents the integrated PSD display of the single sideband noise to 12 kHz for the acoustically shielded circuits. Included are the PM data prior to acoustic shielding and circuit alignment. Each of the spectra shown represents a 0.5-sec time-integrated power spectral density. Levels measured above the system noise are only important within certain bandwidths and during the period of cart acceleration.

rf Interference and Attenuation

Measurments of X-band attenuation and X-band AM/PM noise were made for the second and third firings. Chamber pressure during these tests ranged from 2900 to 3200 psia. The radar cart was held stationary near the exit plane during the initial portion of the test, and then traverses of the downstream regions of the plume were made (Table 1). Attenuation data for the CW, X-band (9.57 GHz) signals were obtained with the lens-corrected AM/PM rocket exhaust radar interferometer. Effects of firing time and plume position on X-band attenuation level are shown in Figs. 4 and 5. Figure 4 indicates that two regions of maximum attentuation occur. One, ~13 in. aft of the exit plane, coincides with the first normal Mach disk, whereas the second occurs in the aft or afterburning regions of the plume. It is possible that shock structure also accounts for the observed fluctuations in the attenuation traces at 40 and 55 in.

During the third firing, the cart was held at 72 in., which closely corresponded to the region of maximum attenuation. The X-band attenuation levels show a gradual decrease with time. Levels measured agree well with those obtained in the moving cart test as shown in Fig. 4 and indicate that afterburning for this propellant formulation is significant. In addition, this agreement provides an indication of the reproducibility.

X-band attenuation measurements made previously[1] at similar conditions are also shown in Figs. 4 and 5. In the moving cart tests, the two programs conducted two years apart show nearly identical peak levels of attenuation. However, during the more recent program the cart had not entirely traversed the exhaust plume before the end of the motor burn period. The reproducibility of the attenuation data during both moving and stationary cart tests, obtained from the two test programs, is shown in Fig. 4 to be within 1 db at a positon 72 in. aft of the nozzle exit plane. Attenuation levels during the stationary tests, shown in Fig. 5, for the 72-in. aft position were again very similar and less than 1 db near the completion of the firings. The higher peak attenuation observed during the initial phase of the earlier motor firing was not observed during the subsequent program. This effect may have been caused by alkali metal impurities in the igniter. Both the lower attenuation levels near the exit plane and the smooth appearance of the curve obtained during the earlier program were caused by the unfavorable microwave beam diameter to exhaust plume diameter.[1] A similar effect accounts for the smoothing action of the large microwave beam across the small normal Mach disks.

AM Noise

Two techniques were used for presenting the AM noise data: PSD plots that show the radar-plume noise data in terms of the spectral density of its mean power value, and noise spectra that present spectral sections of the noise sideband region during a firing. The latter real-time presentation is derived from the recorded data by periodically sampling the entire motor firing-analysis period at discrete frequencies throughout the noise sideband spectral region. Repetitive analysis was provided by operating the recorder in the loop mode whereby a data tape that was originally recorded during the firing is repeated by continuously passing the loop through the reproduce heads.

Figure 6 shows PSD analyses of the spectral region from 500 Hz to 20 kHz for the second and third firings. The spectra were obtained with a 200-Hz analysis bandwidth filter and normalized to 500 Hz. Values shown are referenced to the power of the received carrier. A comparison of lines B and C of Fig. 6, which represent spectra derived from stationary and moving cart tests, respectively, shows that the relatively high levels of AM noise in the afterburning regions of

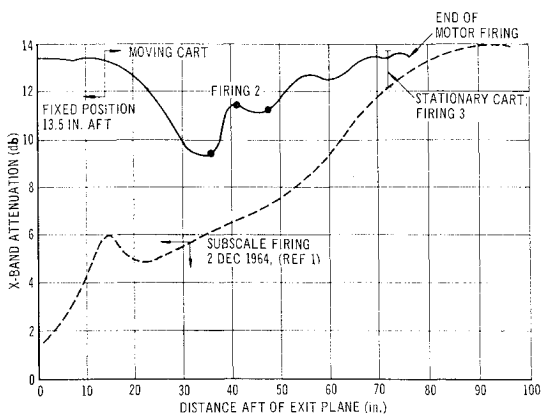

Fig. 4 Effect of plume position on attenuation level.

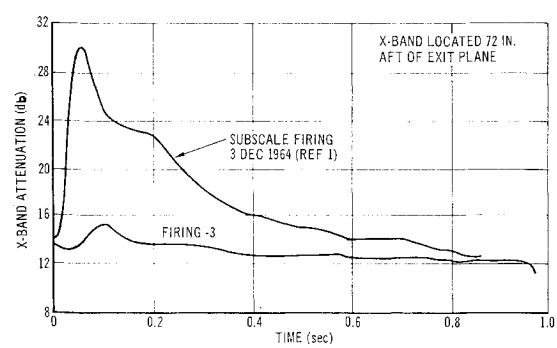

Fig. 5 Effect of firing time on X-band attenuation level.

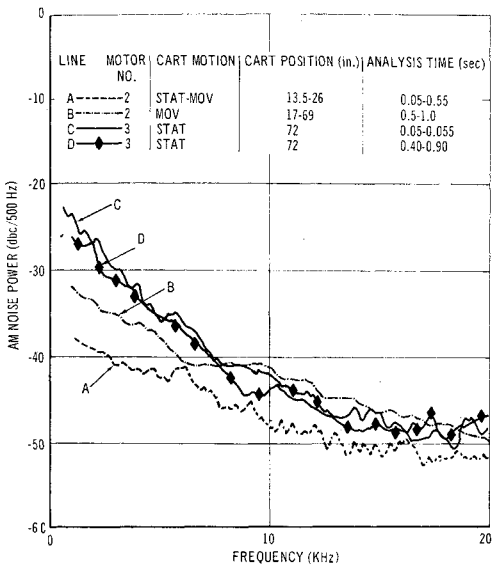

Fig. 6 X-band integrated power spectral density of plume-induced AM noise.

the plume during the scanning test approximates the values obtained with the cart stationary only for sideband frequencies greater than about 10 kHz. At the lower frequencies the noise levels are greater during the stationary firing, the difference being due to a shift of the peak positions of the sideband frequency noise components from the aft regions to an upstream position with an increase of sideband frequency. This results in the different spectral structure of the low-frequency components, shown in Fig. 6 for the scanning and stationary tests. For conditions considered here and later relating to PM noise, an analysis time of 0.5 sec is used that gives rise to a normalized (1 σ) statistical error of about 0.9 db in the 500 Hz to 40 kHz interval.

Effect of plume position on AM exhaust-induced noise for the X-band CW signal is shown in Fig. 7. Maximum noise at all noise-sideband frequencies occurs in the afterburning or aft regions of the plume. For AM noise, a gradual increase in level at all frequencies is observed at the first normal shock followed by a rapid rise that corresponds to the cart traversely scanning the aft regions of the plume. At a noise sideband frequency of 1 kHz, the increase is about 10 db.

The positions of the maximum amplitude noise and attenuation do not always coincide. Low-frequency amplitude noise maximum, for frequencies < 5 kHz, appears to occur near or downstream of the attenuation maximum. However, an increase of the analysis frequency tends to shift the peak noise level upstream toward the nozzle exit plane. At 20 kHz, this shift results in a relatively broad maximum occurring at approximately 10 to 20 exit radii upstream from the location of the maximum observed attenuation level.

PM Noise

Analysis of the recorded demodulated PM video signal followed the same procedures as were discussed for AM noise. Figure 8 shows the PSD single sideband levels for the interval from 0 to 20 kHz. Spectral density plots shown include 0.5-sec analysis intervals wherein the radar cart was either fixed, moving, or both fixed and moving. Included is the system performance for the phase circuit prior to test. The derived phase noise is maximum for the stationary measurements 72 in. aft of the exit plane. Two time intervals were selected for analysis during the stationary test. The first 0.5 sec includes the period immediately after the ignition transient in the plume (0.05–0.55 sec). Line C of Fig. 8 represents another 0.5-sec interval beginning 0.4 sec after ignition. A decrease in phase noise occurs between these two analysis periods. This result closely follows the derived level of X-band attenuation for these periods that also, showed a decrease. The broadband spectral content for stationary and moving radar cart PM spectra are similar.

Figure 7 also shows PM dependence on plume position for the traversely scanning radar beam at X band. Unlike AM noise, maximum PM noise occurs in the aft regions of the plume for only low sideband frequencies. A maximum for the higher frequencies (11–15 kHz) also appeared when the cart was 13 in. aft of the nozzle exit plane (near first shock). In addition, the relative maximum between the first normal shock and afterburning regions for low analysis frequencies show little similarity to their respective counter parts for AM noise. At 1 kHz, a value of 10 db was noted for the level of AM noise increase between the near and aft maximum whereas the corresponding rise for PM noise is only about 1 db. At low frequencies, the maximum PM noise levels appear following the maximum attenuation levels, whereas at higher frequencies the maximum PM noise tends to occur near or upstream of the observed attenuation maximum.

Analysis of Noise Data

Comparisons of the AM and PM noise spectra measured earlier[1] with those of this program (third firing—stationary at 72 in. aft of exit plane) are shown in Fig. 9. For the AM noise, agreement for sideband frequencies between 4 and 10 kHz is excellent. At the lower frequencies, no data were available for the earlier test. Plume-induced noise at frequencies higher than about 20 kHz was not obtained in both test series because of the system noise levels that masked the plume noise in this region.

The PM noise levels were generally higher in the present test series, the difference increasing with increasing sideband frequency. Though no PM noise data were available from the earlier tests for frequencies below 4 kHz, extrapolation would indicate reasonable agreement. As with AM noise, plume-induced PM noise levels above 20 kHz were not obtained. The system noise level obscured the plume effects at the higher frequencies.

The AM noise levels for the test data of this program were comparable to PM noise values; whereas in the earlier test program,[1] AM noise levels were substantially greater than PM values. The present PM noise data are thought to be more reliable than the earlier data.

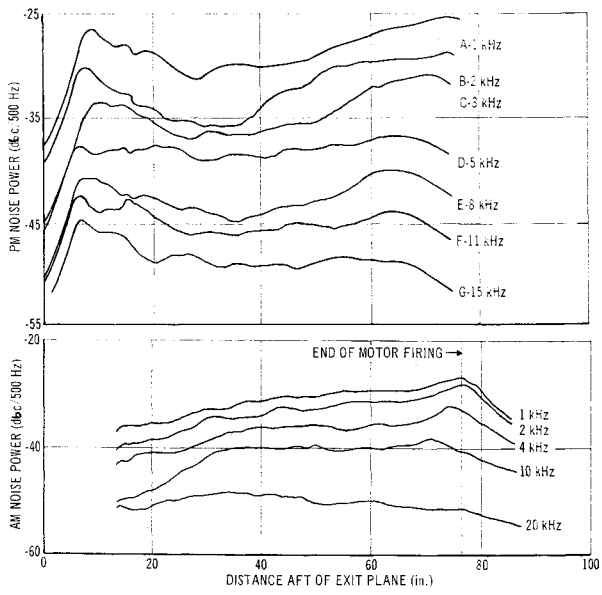

Fig. 7 Effect of sideband frequency and plume position on real-time AM and PM noise spectra.

Techniques for theoretical prediction of radar attenuation[2] were in good agreement with the earlier measured attenuation levels for this propellant/motor system.[1] Techniques for estimating noise levels[3] were also discussed briefly in Ref. 2 and compared with experimental values.

Summary

Limited firing data indicate that the new facility for obtaining the noise and attenuation data is not affected by the mechanical or acoustic disturbances that caused wide excursions of the signal levels during the earlier[1] test program. Although the sets of firings were made over two years apart, measured X-band attenuation levels were comparable. Amplitude and phase noise, however, were similar only within certain sideband frequency intervals, indicating that the unwanted mechanical or acoustic effects, as suggested in Ref. 1, were important.

Both aft regions of the plume and the first normal Mach disc region caused higher levels of PM noise and attenuation than did regions near the exit plane. Relatively high levels of AM noise also occurred in the aft or afterburning plume regions. Like the PM noise and attenuation data, the AM noise values were nearly identical for the same plume position during moving and stationary radar cart tests. The rapid rise that occurred in the AM/PM noise signals as the cart traversely scanned along the exhaust axis was not directly related to similar increase in the attenuation level. The AM noise maximum for the lower sideband frequencies occurred farther downstream than the corresponding attenuation maximum. An increase of the sideband frequency tended to shift the peak position of AM noise upstream. Although the dependence of PM noise levels on plume position were similar to AM noise, some differences were observed. At low frequencies the maximum PM noise level appeared to follow the axial dependence of attenuation, whereas at the higher frequencies PM noise maximums occurred near or upstream from the observed attenuation maximum. Maximum PM noise at the higher frequency, unlike AM noise, occurred near the first normal Mach disk.

The power spectral density distributions of the exhaust plume noise interference data for the broadband frequency intervals were not affected by system noise. High noise levels that occurred at the lower sideband frequencies decreased with increasing frequency. The broadband spectra for the moving and stationary cart tests were similar.

Comparable levels of AM noise for the earlier tests[1] and for this program were obtained for sideband frequencies between 4 and 10 kHz. For higher sideband frequencies that were unaffected by system noise, the earlier measured levels were lower than those reported here. For frequencies less than about 4 kHz, the PM noise levels agreed well with the previous data, although the difference again increases with increasing sideband frequency, with this test series having the higher values. Relative values of AM and PM noise were similar in this test program, whereas measured AM noise levels were substantially higher than PM noise levels in the earlier firings. Moreover, the PM noise levels did not have the wide excursions noted during the earlier firings. These later findings are considered more reliable because of the careful attention given to reducing acoustically induced noise levels.

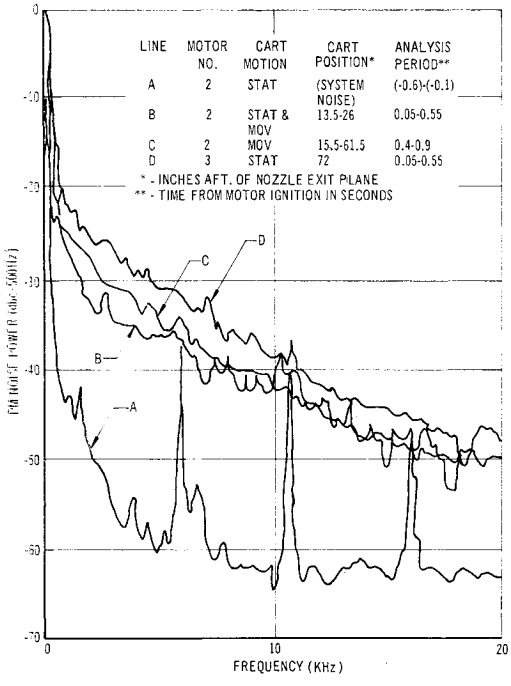

Fig. 8 X-band integrated power spectral density of plume-induced PM noise.

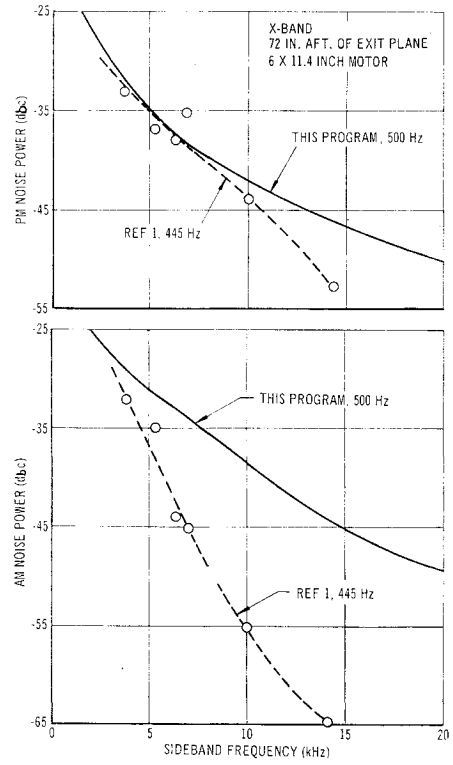

Fig. 9 Comparison of AM and PM noise levels for identical motors from two test programs using different test facilities.

References

[1] Smoot, L. D. and Seliga, T. J., "Rocket Exhaust Plume Radar Attenuation and Amplitude/Phase Noise," *Journal of Spacecraft and Rockets*, Vol. 4, No. 6, June 1967, pp. 774–780.

[2] Smoot, L. D. and Underwood, D. L., "Prediction of Microwave Attenuation Characteristics of Rocket Exhausts," *Journal of Spacecraft and Rockets*, Vol. 3, No. 3, March 1966, pp. 302–309.

[3] Geiger, A. A., "Analysis of the Effects of Rocket Exhaust Fluctuations," AIAA Paper 65-184, Washington, D. C., 1965.